Available online at www.sciencedirect.com
ScienceDirect
Materials Letters 62 (2008) 1139–1142
materials letters
www.elsevier.com/locate/matlet

Effect of Mg addition on the τ phase distribution of an AlMn alloys modified with zinc

S. Valdez [a,*], J. Genescá [b], B. Campillo [a], O. Flores [a], R. Pérez [a], J.A. Juárez-Islas [c]

[a] Instituto de Ciencias Físicas-UNAM, Av. Universidad S/N, Col. Chamilpa, 062210, Cuernavaca, Morelos, México
[b] Facultad de Química, Cd. Universitaria, 04510, México, D.F., México
[c] Instituto de Investigaciones en Materiales-UNAM, Circuito escolar S/N, Cd. Universitaria, 04515, México, D.F., México

Received 22 May 2007; accepted 1 August 2007
Available online 7 August 2007

Abstract

The effect of Mg addition on the τ phase formation of an AlMn alloys modified with Zn, has been investigated by means of X-ray diffraction, scanning electron microscopy and transmission electron microscopy, complemented by micro vickers hardness and galvanic efficiency. The results show the τ precipitates are formed when aged at 450 °C for 5 h in AlMnZn–(Mg) alloy with upper to 5.49% Mg addition. The hardness and galvanic efficiency value of the aged alloy with 5.49% Mg is always distinctly higher than that of the alloy in as-cast condition with the same composition. Based on microstructural and galvanic efficiency results the quantity of τ phase with Mg addition is discussed, in order to relate the τ distribution with the galvanic efficiency.

Keywords: AlMnZn–(Mg) alloy; τ-phase; Galvanic efficiency

1. Introduction

AlMnZn–(Mg) based alloys are widely used in aerospace applications due to the unique combination of lightweight and high mechanical properties [1–5]. However, recently the AlMnZn–(Mg) alloy has been pointed out as a promising alloy system to be studied due to its low electrode potential, high current capacity to be used as galvanic anode [3,6]. A lot of effort has been spent on investigation of precipitation process in AlMnZn–(Mg) alloys [7–10], as these are commercially important. It has been known for some years that several transformation sequences may occur in these materials during ageing [4]. It is well known that the microstructure is essential for the properties of alloys. Magnesium is the most active metal in the galvanic series and magnesium alloy component is always the active anode if it is in contact with other metals [8,11]. In this study, the effects of Mg addition on the microstructure and galvanic efficiency of AlMnZn–(Mg) alloys were investigated. The aim of the present study was to understand better the role played by Mg on the τ particles distribution which produces the activation anodic process related with the galvanic efficiency of the alloy.

2. Experimental procedure

AlMnZn–(Mg) alloys were prepared by casting from commercial purity materials. The samples were homogenized at 450 °C for 5 h and quenched in water. Homogenized samples were aged at 400 °C for 1 h. Alloying elements contents were analyzed by using ICP method. Chemical analyses results are given in Table 1. As-cast and aged samples were sectioned longitudinally at mid-width using a band saw. One side was prepared for microstructural characterization by grinding on SiC metallographic paper, polishing with 0.5 and 0.05 μm alumina power and etched with Keller's reagent. Microstructures were studied using a Stereoscan 440 scanning electron microscope using backscattered electron imaging (SEM) operated at 20 kV and a Jeol 2100 scanning transmission electron microscope

* Corresponding author. Tel.: +52 55 56227785; fax: +52 55 56227734.
E-mail address: svaldez@fis.unam.mx (S. Valdez).

0167-577X/$ - see front matter © 2007 Elsevier B.V. All rights reserved.
doi:10.1016/j.matlet.2007.08.001

Table1
Composition of AlMnZn–(Mg) alloy under study, given in wt.%

Alloy	Al (%)	Mg (%)	Zn (%)	Mn (%)	Other elements
1	90.2461	3.96	5.36	0.3189	0.1150
2	89.3885	4.89	5.35	0.3125	0.1390
3	88.7560	5.49	5.32	0.3053	0.1287
4	87.7416	6.55	5.32	0.2320	0.1564
5	87.9500	7.33	5.30	0.2931	0.1269
6	85.6380	8.65	5.29	0.2877	0.1343
7	84.7427	9.58	5.29	0.2851	0.1022
8	82.8194	11.53	5.31	0.2178	0.1228

(TEM). Both equipped with an in situ energy dispersive spectrometer (EDS). The TEM foils were taken from the mid-point of each sample at the centre of the cross-sections. Structural investigations were carried out by X-ray diffraction (XRD) using a Siemens D5000 by employing a Cu Ka radiation, a Ni filter and a scan velocity of 2°/min. The Vickers hardness was measured on the cross-sections of the samples using a load of 2 N. The test anode and cathode were coupled together and immersed in 3% NaCl solution for 4 days. The weight of the anode before and after the immersion was measured after cleaning the anodes (ASTM G 31). From the actual weight loss measured, the theoretical current to be produced by the alloy could be calculated. Galvanic efficiency = (*S*/*C*)(100), where *S* is de actual current produced in the system, and *C* is the theoretical current to be produced by the system as from Faradays laws.

3. Results and discussion

Fig. 1 shows the X-ray diffraction patterns taken of the AlMnZn–(Mg) specimens, in as-cast and ageing condition. This figure shows that the alloys in as-cast condition and aged are composed of α-Al solid solution and τ-$Al_2Mg_3Zn_3$ precipitates (τ-phase particles) when the Mg addition is up to 5.49% Mg. One phase precipitation is suggested by the progressive shifting of (530) yr (100) X-ray diffraction peaks of τ phase, from 2θ angles of 36.71–35.3° yr 8.80–6.58°, formed up to 7.33% Mg content (Fig. 1a).

The X-ray diffractograms (left side) in as-cast and aged condition show that τ-$Al_2Mg_3Zn_3$ precipitates are formed at high Mg addition but there are few reflections of the τ precipitates for the low Mg sample shown in Fig. 1 (right side). These observations demonstrate that the formation of the τ-phase particles was promoted through the high Mg addition with aged condition. It is apparent also from inspection of Fig. 1 (right side) that the relative intensities for the (111) reflection of the α-Al (which is a rich aluminum solid solution of crystalline structure fcc) is much higher than the other peaks, thereby indicating the presence of a texture was developed during the casting operation. During the heat treatment an atomic reordering of the aluminum matrix exists towards a preferential direction of the planes (220) and (311) as it can be observed in Fig. 1c. The variations in intensity and small displacements of the diffraction angle have their origins due to the variations in composition of the alloy.

Fig. 2 shows the microstructure of as-cast and aged AlMnZn–(Mg) alloys. As-cast structure is modified with heat treatment. It can be observed that dendritic structure is broken down and show a quasibinary eutectic mixture of Al and $Al_2Mg_3Zn_3$ present along the grain boundaries of primary α-Al grains in aged alloys (Fig. 2a). In the eutectic region the light contrast corresponds to $Al_2Mg_3Zn_3$, while dark

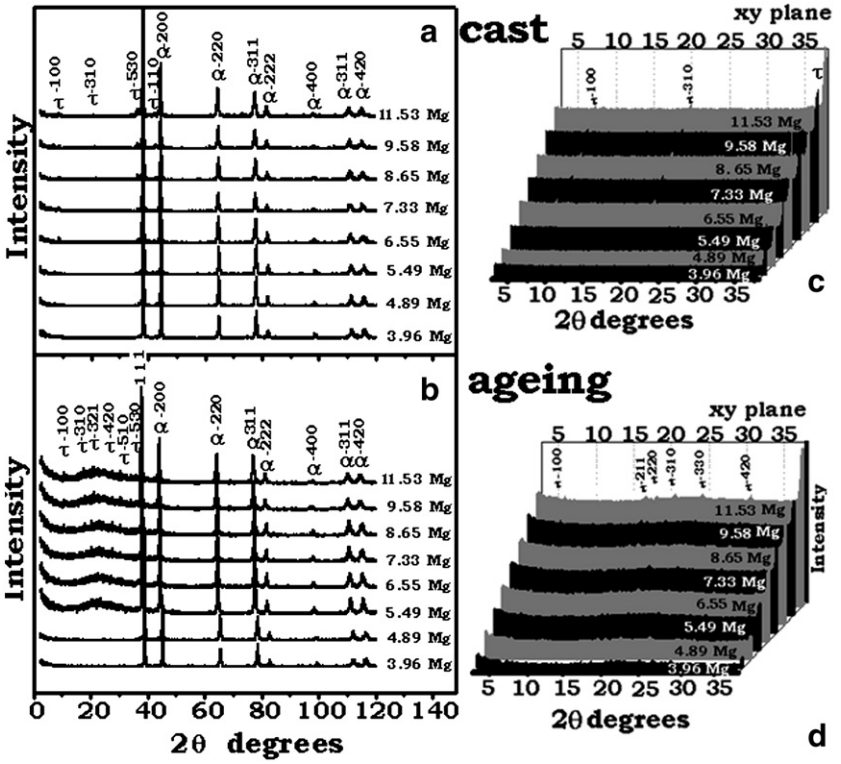

Fig. 1. X-ray diffractograms of the AlMnZn–(Mg) alloy in as-cast condition showing the presence of the main lines of diffraction τ-$Al_2Mg_3Zn_3$ and α-Al peaks with eight different Mg content.

contrast corresponds to the α-Al phase. It has been reported [2,9] that the lamellar eutectic structure is derived from the decomposition of the α' phase by the following cellular reaction at 762 K, $\alpha' \rightarrow \alpha\text{-Al} + \tau\text{-}Al_2Mg_3Zn_3$ (τ; bcc, $a = 1.416$ nm, Im3). Homogeneously dispersed stable τ rods precipitates of 3 μm length in aged samples were observed (Fig. 2a). The heat treatment and high Mg addition caused and increase of the volume fraction of $\tau\text{-}Al_2Mg_3Zn_3$ precipitates. The literature on alloys [12, 13] of the type studied in this work, point out that the equilibrium situation involves the existence of an aluminum based α-solid solution and another phase (τ) having a variable composition around the $Al_2Mg_3Zn_3$ formula.

The as-cast microstructure alloys (Fig. 2b) reveals the presence of equiaxed dendritic structure with dendrite arm spacing about 20–30 μm. The TEM micrograph shown in Fig. 2(c) is representative of the microstructures of the $\tau\text{-}Al_2Mg_3Zn_3$ phase present in aged alloy preferentially. The average sizes of these particles were measured as 2 and 3 μm for the AlMnZn–(Mg) cast and ageing alloys respectively. The indexing of the diffraction pattern (Fig. 2d) shows that the lattice parameters of the precipitates are congruent to Al_2Mg_3Zn [14,15].

Microhardened and galvanic efficiency curves in as-cast and aged condition are shown in Fig. 3. The α-Al aged structure is 8% harder than the surrounding Al-matrix in as-cast alloys. Indeed, the average Vickers hardness measured inside the Al-matrix in cast structure is 83.65 HV, whereas the Al-matrix aged is 91.81 HV. These values emphasize the influence of the τ-phase particles inside the matrix. As reported [15,16] precipitates active the alloy surface and influenced in electrochemical efficiency when it breakdown the oxide film formed in air that cover the surface of the α-AlMnZn–(Mg) alloy. It can be seen from Fig. 3 that the alloy with 5.49% Mg addition had a greatly hardening and galvanic efficiency which developed at 1.0 vol% τ-phase particles. The peak efficiency is achieved after 4.89% Mg addition. The efficiency curve for as-cast condition show the similar behavior: the high peak is reached when τ-phase is equal to 1.0 vol. %. It is clear that aging treatment enhance the peak hardness and efficiency when Mg addition does not exceed 5.49%. It means that τ phase

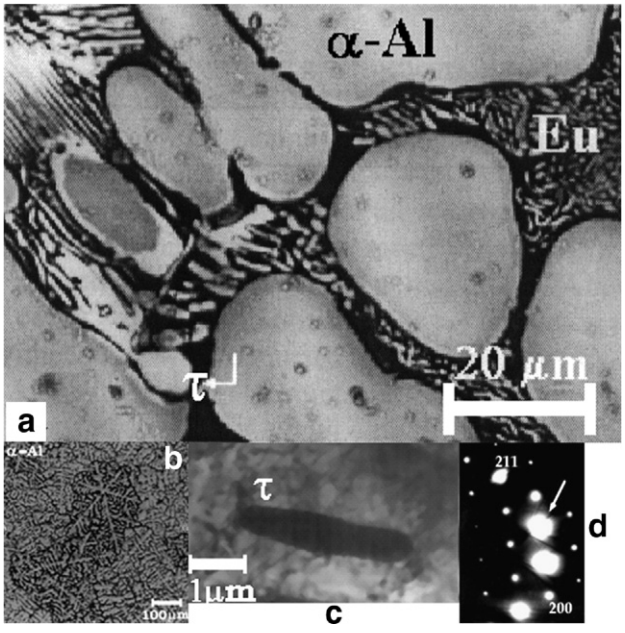

Fig. 2. Shows the microstructure of AlMnZn–(Mg) alloys. (a) τ precipitation in the matrix aged condition, (b) α-Al equiaxed dendritic structure as-cast condition, (c) τ precipitates and (d) relative electron diffraction pattern, it can be indexed according to a body cubic center crystalline structure ($a = 1.416$ nm).

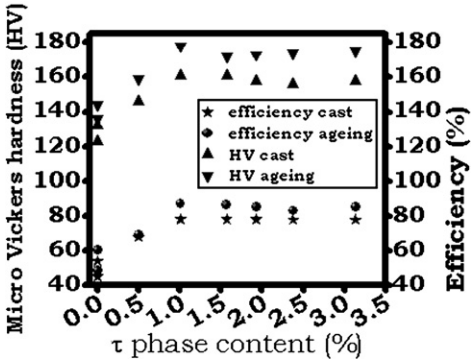

Fig. 3. Hardness/efficiency-τ phase curves for the alloys AlMnZn–(Mg) in as-cast and aged condition.

increase due to the formation of quasibinary eutectic structure (α-Al + τ-$Mg_3Zn_3Al_2$) while the α-matrix decreases and also its τ precipitate distribution. In addition, the efficiency is greater when the initial attack is present for the intermetallic compounds (τ-particles) distributed in the matrix, however the intergranular eutectic phase begins to dissolve it and this intergranular corrosion is stronger than the τ-phase a similar event has been report by Weilong and Frankel [17].

4. Conclusions

According to the effects of Mg addition on the microstructure and galvanic efficiency of an AlMn alloys modified with Zn, the following conclusions are obtained:

i. The precipitation of τ particles depends on the Mg addition, ageing condition and the quantity of the eutectic phase formation.
ii. The addition of Mg in just 5.49 at.% to the ageing AlMnZn alloy clearly increases the peak efficiency and generate the 1.0 vol.% of τ precipitates.
iii. For Mg content upper than 5.49% with ageing condition the eutectic phase increase more than τ precipitates, and the efficiency of the alloy decrease while for low magnesium content the τ phase is poor such as efficiency.
iv. A galvanic efficiency as high as 81% has been achieved with Mg and aged on AlMnZn–(Mg) alloy, that activation process depends on the amount of τ particles deposited at the Al-matrix surface.

Thus, it is concluded that Al–Mn–5.3Zn–5.49Mg alloy are economical, convenient to prepare and apply and highly efficient as sacrificial anode.

References

[1] A.V. Sameljuk, O.D. Neikov, A.V. Krajnikov, Yu.V. Milman, G.E. Thompson, X. Zhou, Corros. Sci. 49 (2007) 276–286.
[2] F. Mondolfo, Metall. Rev. 16 (1971) 953.
[3] E.H. Hollingsworth, H.Y. Hunsicker, Corrosion, nineth ed, Metals Handbook, vol. 13, Am. Soc. For Metals, Metals Park, Ohio, 1987, pp. 583–609.
[4] H. Cordier, C. Dumond, W. Gruhl, Metallurgy 34 (1980) 515.
[5] I.J. Polmear, J. Inst. Met. 89 (1960) 51.
[6] A. Barbucci, G. Cerisola, G. Bruzzone, A. Saccone, Electrochim. Acta 42 (1997) 2369.

[7] T. Engdahl, V. Hansen, P.J. Warren, K. Stiller, Mater. Sci. Eng., A Struct. Mater. Prop. Microstruct. Process 327 (2002) 59–64.
[8] S.K. Maloney, K. Hono, I.J. Polmear, S.P. Ringer, Scr. Mater. 41 (10) (1999) 1031.
[9] K. Hono, N. Sano, T. Sakurai, Surf. Sci. 266 (1992) 350.
[10] P.J. Warren, C.R.M. Grovenor, J.S. Crompton, Surf. Sci. 266 (1992) 342.
[11] Guangling Song, Birgir Johannesson, Sarth Hapugoda, David StJohn, Corr. Sci. 46 (2004) 955–977.
[12] J.B. Clark, Trans. Am. Soc. Met. 53 (1961) 295.
[13] G.M. Kuznetsov, A.D. Barsukov, G.B. Krivoshuva, E.V. Barshashkina, Izv. Akad. Nauk. SSSR Met. 4 (1986) 198.
[14] J.H. Ault, B.E. Williams, Acta Crystallogr 21 (1966) 830.
[15] A. Barbucci, P.L. Cabot, G. Bruzzone, G. Cerisola, J. Alloys Comp. 268 (1998) 295–301.
[16] S.M.A. Shibli, V.S. Gireech, App. Surface Sci. 219 (2003) 203–210.
[17] Weilong Zhang, G.S. Frankel, Electro. Acta 00 (2003) 1–18.